

Effect of post-annealing on structural and electrochromic properties of Mo-doped V_2O_5 thin films

**W. Yong, H. L. Zhang, H. T. Cao,
T. Tian, J. H. Gao, L. Y. Liang & F. Zhuge**

**Journal of Sol-Gel Science and
Technology**

ISSN 0928-0707
Volume 77
Number 3

J Sol-Gel Sci Technol (2016) 77:604–609
DOI 10.1007/s10971-015-3889-8



Your article is published under the Creative Commons Attribution license which allows users to read, copy, distribute and make derivative works, as long as the author of the original work is cited. You may self-archive this article on your own website, an institutional repository or funder's repository and make it publicly available immediately.

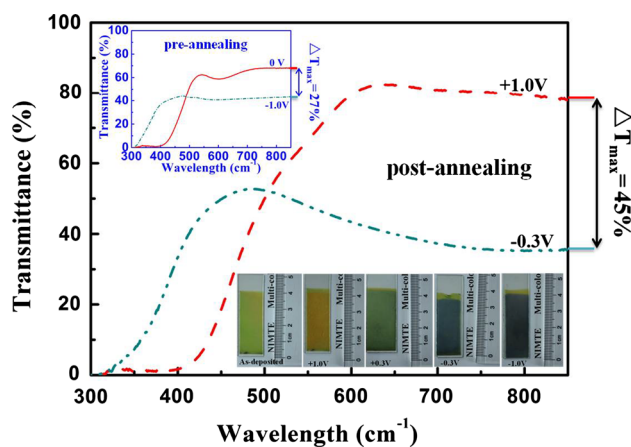
Effect of post-annealing on structural and electrochromic properties of Mo-doped V_2O_5 thin films

W. Yong^{1,2} · H. L. Zhang² · H. T. Cao² · T. Tian² · J. H. Gao² · L. Y. Liang² · F. Zhuge²

Received: 13 July 2015 / Accepted: 5 October 2015 / Published online: 12 October 2015
© The Author(s) 2015. This article is published with open access at Springerlink.com

Abstract The effect of post-annealing on the structural and electrochromic properties of the Mo-doped V_2O_5 thin films was investigated in this paper. With varying the annealing temperature, the interlayer distance is increased from 1.16 (as-deposited) to 1.38 nm (annealing at 250 °C), and the enlarged interlayer spacing would facilitate ion movement in between the interlayers inside the electrochromic matrix. Therefore, both the optical modulation and color efficiency of the Mo-doped V_2O_5 thin films are enhanced after appropriate post-annealing treatment. Our results demonstrate that Mo-doped V_2O_5 material is one of the promising candidates to be used in multi-color electrochromic devices.

Graphical Abstract The ability to modulate optical transmittance of the Mo-doped V_2O_5 thin films is greatly enhanced by means of the larger interlayer distance after annealing.



Keywords Multi-color electrochromic · V_2O_5 thin films · Post-annealing

1 Introduction

The electrochromic (EC) thin films have drawn great attentions over the past 50 years due to their numerous applications such as smart windows, auto rearview mirrors, large-area displays, color glasses, and space shuttles [1–5]. In particular, electrochromic material-based devices have multiple advantages such as low-voltage operation, low-energy consumption, low-carbon green, and memory effect without power supply. Organic or transition metal oxide thin films are commonly used as the electrochromic layers. For example, Shaplov et al. [6] have reported all-polymer-based electrochromic devices (ECDs) using polymeric ionic liquids and poly (3,4-ethylenedioxythiophene) (PEDOT) thin films as the ion conductor and EC layers,

Electronic supplementary material The online version of this article (doi:10.1007/s10971-015-3889-8) contains supplementary material, which is available to authorized users.

✉ H. L. Zhang
zhanghl@nimte.ac.cn

✉ H. T. Cao
h_cao@nimte.ac.cn

¹ Department of Chemical and Environmental Engineering, North University of China, Taiyuan 030051, People's Republic of China

² Ningbo Institute of Material Technology and Engineering, Chinese Academy of Sciences, Ningbo 315201, People's Republic of China

respectively, demonstrating fast switching time (3–5 s), high coloration efficiency (up to $430 \text{ cm}^2/\text{C}$), and satisfactory optical contrast (up to 28.5 %). Recently, organic ECDs composed of poly(1,4-bis(2-(3,4-ethylenedioxythiophene))naphthalene) and poly(2,6-bis(2-(3,4-ethylenedioxythiophene))naphthalene) have been constructed [7], exhibiting reasonable optical contrasts and fast response time. However, organic electrochromic materials are always limited by long-term reliability, which is the bottleneck for real applications [8, 9]. Alternatively, transition metal oxides such as tungsten, vanadium, titanium, molybdenum, and nickel oxides could circumvent such circumstance. Among these inorganic materials, vanadium oxide thin films have been gained great interests, owing to their multi-color electrochromic behaviors [10]. V_2O_5 thin films can be fabricated using either physical vapor deposition techniques (such as magnetron sputtering [11], pulsed laser deposition [12]), or solution-based techniques (such as sol-gel [13], spin coating [14], and electrochemical deposition). Structural and EC properties of the V_2O_5 thin films depend not only on the deposition parameters but also post-annealing processes. For instance, it was demonstrated that [15] annealing treatment has a great impact on the optical and microstructural properties of the nanocrystalline V_2O_5 thin films. The annealing-induced (at $500 \text{ }^\circ\text{C}$) pore structure could improve the charge/discharge rate efficiently. A multi-color electrochromic Mo-doped V_2O_5 thin films with layered structure had been successfully prepared via electrochemical deposition method [16]; however, the effect of post-annealing on structural and electrochromic properties of the Mo-doped V_2O_5 thin films has not been clarified yet.

In this paper, the effect of post-annealing on the structural and electrochromic properties of the Mo-doped V_2O_5 thin films was investigated. The Mo-doped V_2O_5 thin films were characterized by X-ray diffraction (XRD), Raman spectra, electrochemical workstation, and UV-Vis-IR spectroscopy. It was revealed that the annealing process is indispensable to improve the optical and electrochemical properties of the EC films.

2 Experimental

The Mo-doped V_2O_5 thin films were prepared by electrochemical deposition, as reported elsewhere. [17] The ITO-coated glass and the platinum foil were used as the working electrode and counter electrode, respectively. The Mo-doped V_2O_5 thin films were deposited potentiostatically by applying a fixed potential of -0.3 V . After deposition, the thin films were dried in air at room temperature. The as-deposited Mo-doped V_2O_5 thin films were annealed in air

at different temperatures of 150, 200, 250, and $300 \text{ }^\circ\text{C}$ for 2 h and then cooled down naturally.

The microstructure and optical properties of the Mo-doped V_2O_5 thin films were analyzed by X-ray diffraction [XRD, Bruker D8 Advance using $\text{Cu-K}\alpha$ ($\lambda = 0.154178 \text{ nm}$) radiation and a theta-2theta configuration], high-resolution transmission electron microscopy (HRTEM, JEOL2100), Raman spectra (Renishaw in Via Raman Microscope using excitation laser with wavelength of 633 nm), and UV-Vis-IR spectroscopy (PerkinElmer Lambda 950), respectively. The cyclic voltammetry measurement was taken in a potential range from $+1.0$ to -1.0 V with a scan rate of 50 mV s^{-1} . 0.1 M LiClO_4 dissolved in propylene carbonate was used as the electrolytic solution. The thin films were polarized by applying voltage at $+1.0$, $+0.3$, -0.3 , and -1.0 V for 40 s, respectively. The impedance spectra were measured on an electrochemical workstation (Zennium, IM6), covering the frequency range from 100 mHz to 10 kHz.

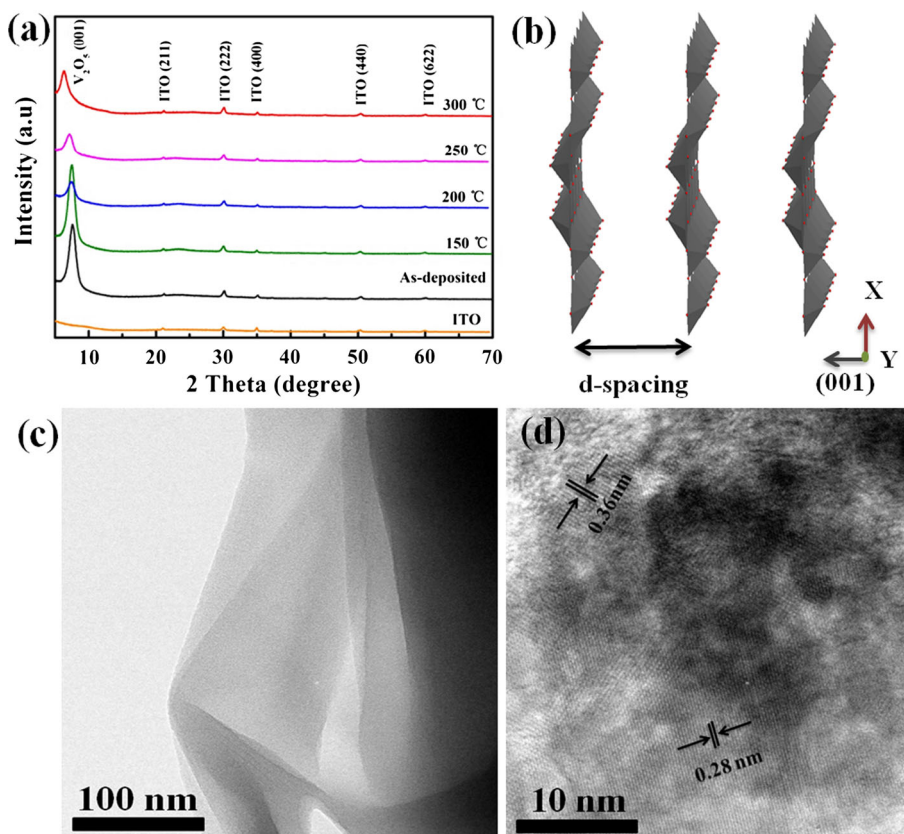
3 Results and discussion

Figure 1a shows the XRD patterns of the Mo-doped V_2O_5 thin films on ITO-coated glass. The (001) peak of the as-deposited Mo-doped V_2O_5 thin film is located at 7.6° , while that of the Mo-doped V_2O_5 thin films annealed at 150, 200, 250, and $300 \text{ }^\circ\text{C}$ is centered at 7.4° , 7.2° , 7.1° , and 6.4° , respectively. Moreover, with increasing the annealing temperature, the (001) peak of the Mo-doped V_2O_5 thin films is further shifted to the lower angles. The (001) preferred orientation reveals that the Mo-doped V_2O_5 thin films have a layered structure, which is beneficial for ion injection and extraction [18, 19]. Besides, the diffraction peaks located at 21.3° , 30.0° , 34.8° , 50.4° , 60.1° are attributed to polycrystalline ITO. The interlayer distance of the Mo-doped V_2O_5 can be calculated by the Bragg formula [20]:

$$2d \sin \theta = n\lambda, \quad (1)$$

where d is the interlayer distance, and θ , n , and λ the diffraction angle, the diffraction order, and the wavelength of the X-ray, respectively. The interlayer distance of the as-deposited Mo-doped V_2O_5 thin film is calculated to be 1.16 nm, while that of the Mo-doped V_2O_5 thin films annealed at 150, 200, 250, and $300 \text{ }^\circ\text{C}$ is 1.20, 1.22, 1.25, and 1.38 nm, respectively. These results are consistent with the previous report [21]. It is obvious that the interlayer distance is increased after annealing treatment. In addition, the (001) peak intensity of the annealed Mo-doped V_2O_5 thin films is attenuated with respect to the as-deposited ones, which is in a good agreement with the previous reports [17, 22]. The layered structure model of V_2O_5 along

Fig. 1 **a** XRD patterns of the as-deposited Mo-doped V_2O_5 films and the annealed films at different temperatures. **b** Layered structure model of V_2O_5 along the (001) direction. **c** TEM and **d** HRTEM images of the 250 °C-annealed Mo-doped V_2O_5 thin films



the (001) direction is illustrated in Fig. 1b. Base-faced square-pyramidal V_2O_5 units are arranged in parallel with an equal distance (d-spacing), as reported elsewhere [23]. The detailed morphologies of the 250 °C-annealed Mo-doped V_2O_5 thin films are further investigated by TEM analysis, as presented in Fig. 1c, d. The layered structure of the thin films is shown in Fig. 1c. Similar results have also been observed for the layered Al-doped WO_3 thin films [24]. The HRTEM image (Fig. 1d) of the thin film presents clear fringes with a fringe spacing of 0.28 and 0.36 nm, corresponding to the interplanar distance of (004) and (003) lattice planes of V_2O_5 (JCPDS # 52-0794), respectively. Because the (004) and (003) peaks of the V_2O_5 are broad and weak, or overlapped with the peak of crystalline ITO (located at 34.8°), so the (004) and (003) peaks of the V_2O_5 are not observed in the XRD results.

Raman spectra of the thin films are illustrated in Fig. 2. The peaks centered at 160, 266, 326, 511, 704, and 879 cm^{-1} for the as-deposited Mo-doped V_2O_5 films are attributed to the $V-O_x$ bonds and $V-O-Mo$ bonds. The Raman peaks of the 250 °C-annealed Mo-doped V_2O_5 films are located at 162, 271, 328, 514, and 707 cm^{-1} , which are also corresponding to the $V-O_x$ and $V-O-Mo$ modes. The Raman peak shift (about +2 to +5 cm^{-1}) after annealing is believed to be due to the enhancement of the element diffusion and the variation in interatomic forces, which is

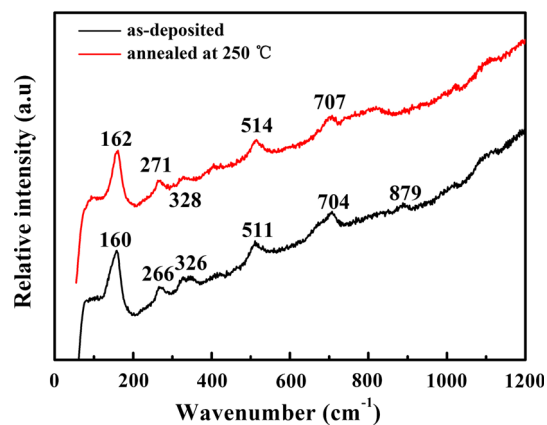


Fig. 2 Raman spectra of the as-deposited and 250 °C-annealed Mo-doped V_2O_5 thin films

coupling with the increase in the interlayer distance. In fact, as reported previously [25], the annealing treatment would trigger phase transition from VO_2 to V_2O_5 due to the atom diffusion enhancement. In our case, no stretching vibration mode of $V^{4+}-O-V^{4+}$ located at 879 cm^{-1} is observed for the Mo-doped V_2O_5 thin films annealed at 250 °C, in line with the previous literatures [26, 27].

Figure 3 displays the cyclic voltammograms for the Mo-doped V_2O_5 thin films annealed at 250 °C. There is no

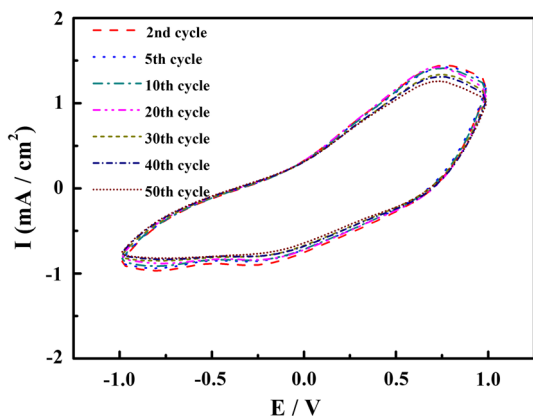


Fig. 3 Cyclic voltammograms of the 250 °C-annealed Mo-doped V₂O₅ films. The voltammograms were recorded with a 50 mV/s scan rate from 1st to 50th cycle

obvious difference in the voltammetric responses of the 2nd, 5th, 10th, 20th, 30th, 40th, and 50th voltammetric cycle. During the voltammetric measurement, the Mo-doped V₂O₅ thin films display multi-color electrochromic behaviors, i.e., red–orange, dark green, blue, and purple blue façade are clearly observed, as reported elsewhere [28]. Enhanced intervalence charge transfer between Mo⁶⁺ and V⁵⁺/V⁴⁺ states owing to the Mo-doping effect, along with the charge transfer between V⁵⁺ and V⁴⁺, can account for the multi-color electrochromic characteristics of the Mo-doped V₂O₅ thin films.

Transmittance spectra and digital photographs of the Mo-doped V₂O₅ thin films in different coloration states are demonstrated in Fig. 4. The neutral form (at 0 V) of the 250 °C-annealed Mo-doped V₂O₅ thin films is yellow in color. Stepwise oxidation of the Mo-doped V₂O₅ thin films shows that the color is varied from purple blue (–1.0 V) to red–orange (+1.0 V), while blue (–0.3 V) and dark green (+0.3 V) are also present at the intermediate state. The transmittance variation in the as-deposited Mo-doped V₂O₅ thin films is determined to be ranging from 18 to 27 % in the spectral region of 600–850 nm. The maximal transmittance difference (ΔT_{\max}) [20] at 850 nm between the bleached state and colored state is calculated to be 27 % for the as-deposited specimen. In comparison, the transmittance variation in the 250 °C-annealed Mo-doped V₂O₅ thin film is ranging from 20 to 45 % in the spectral region of 600–850 nm, and the ΔT_{\max} at 850 nm is 45 %, which is comparable with the previous literatures [29, 30]. The better performance of the annealed thin films is believed to be due to a larger amount of Li⁺ ions and electrons available to be involved into the electrochemical process, in which the layered structure affords an opportunity for the ions and electrons to be intercalated and deintercalated more easily and reversibly.

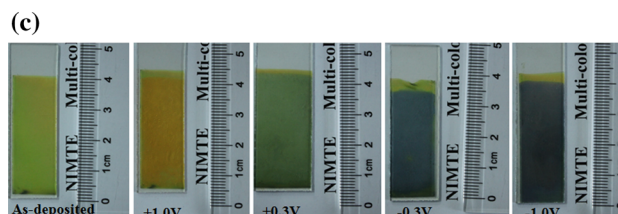
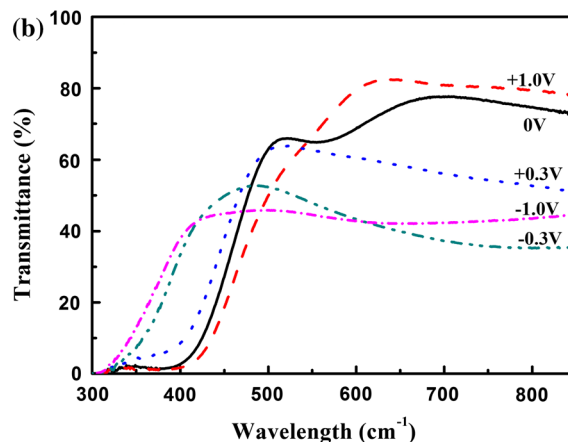
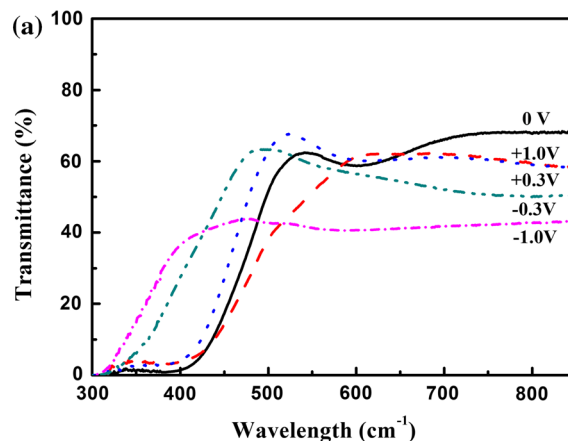


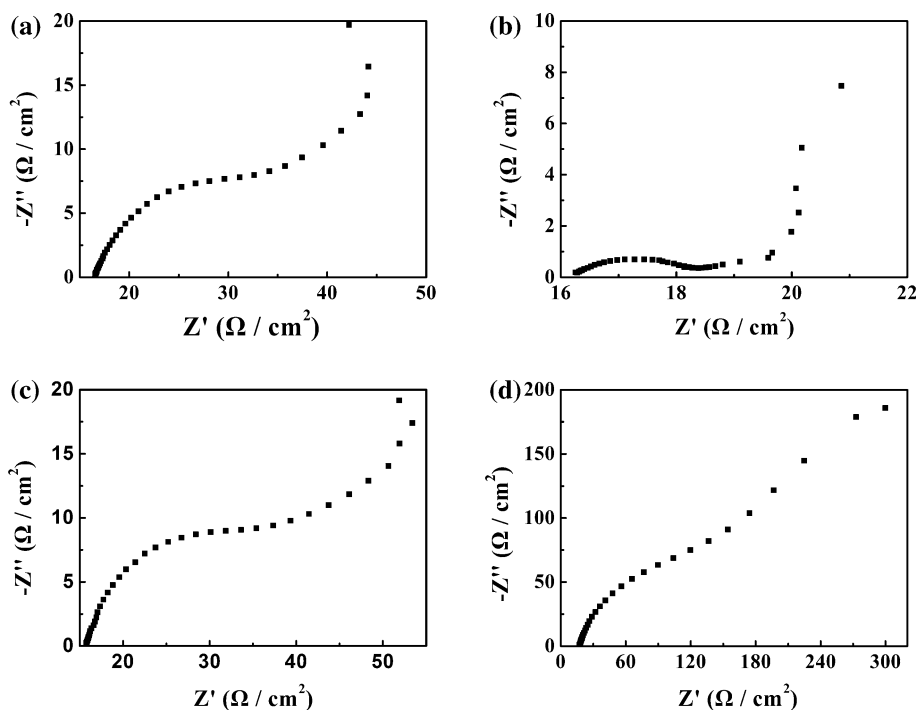
Fig. 4 Transmittance spectra of the Mo-doped V₂O₅ thin films **a** as-deposited and **b** annealed at 250 °C. **c** Digital photographs of the 250 °C-annealed Mo-doped V₂O₅ thin films at various coloration states

Another important criterion for the electrochromic materials is coloration efficiency (η), which is defined as the optical density change in response to the stored charge per unit area (i.e., square centimeter) during the coloration process, as expressed in the following equation [31]:

$$\eta = \Delta OD/q = \log(T_{\text{bleached}}/T_{\text{colored}})/q, \tag{2}$$

where ΔOD is the change in optical density, q is inserted (extracted) charge per unit area, and T_{bleached} and T_{colored} are the transmittance of the film in the bleached state and in the colored state, respectively. The coloration efficiency of the as-deposited and annealed Mo-doped V₂O₅ thin films is calculated to be ~ 22.2 and ~ 42.7 cm² C⁻¹, respectively.

Fig. 5 Impedance spectra of the 250 °C-annealed Mo-doped V_2O_5 thin films at different potentials in 0.1 M solution of $LiClO_4$ dissolved in propylene carbonate. **a** ± 1.0 V, **b** ± 0.3 V, **c** -0.3 V, **d** -1.0 V



For the annealing case, the higher coloration efficiency is consistent with the larger optical modulation.

Figure 5 displays the Nyquist plots of the 250 °C-annealed Mo-doped V_2O_5 thin films at a potential of +1.0, +0.3, -0.3 , and -1.0 V. The charge transfer and the Li^+ ions transport in the electrochemical process are described by the Nyquist plots as follows.

At +1.0 V (Fig. 5a), the Mo-doped V_2O_5 thin films have an oxidation state, which is mainly composed of V^{5+} centers [31]. Thus, the Mo-doped V_2O_5 thin films show a capacitive semicircle in the high-frequency region and diffusion behavior in the low-frequency domain. At the potential of +1.0 V, partial V^{5+} ions are gotten reduced along with the extraction of Li^+ ions from the Mo-doped V_2O_5 layers, resulting in a red–orange color. At +0.3 V (Fig. 5b), a part of V^{5+} ions in the Mo-doped V_2O_5 thin films are further reduced, displaying a dark green color. In this case, a capacitive semicircle in the high-frequency range and a straight line close to 90° at the low frequency are obtained, suggesting that the electrochemical reaction kinetics is controlled by the charge transfer between V^{5+} and V^{4+} at high frequencies. At -0.3 V (Fig. 5c), the plot exhibits a capacitive semicircle in the high-frequency region and a diffusion behavior in the low-frequency domain, similar to the plot at the potential of +1.0 V. The charge-transfer resistance of the Mo-doped V_2O_5 thin films at -0.3 V is higher than that at +1.0 V. At -1.0 V (Fig. 5d), the plot demonstrates a semicircle in the high-frequency region and a linear Warburg region in the low-

frequency region, which corresponds to the charge transfer and ion diffusion, respectively. This indicates that a larger number of V^{5+} are reduced into V^{4+} , and then, V^{4+} centers are formed in the Mo-doped V_2O_5 thin films [28].

4 Conclusions

In summary, the effect of post-annealing on the structural and electrochromic properties of the Mo-doped V_2O_5 thin films was discussed. The optimum annealing temperature in our study was found to be 250 °C. In comparison with the as-deposited state, the interlayer distance was increased from 1.16 to 1.38 nm after annealing at 250 °C, which facilitates the reversible intercalation and deintercalation of Li^{\pm} ions. Resultantly, the coloration efficiency of the Mo-doped V_2O_5 thin films annealed at 250 °C was $42.7 \text{ cm}^2 \text{ C}^{-1}$, while that of the as-deposited thin films was $22.2 \text{ cm}^2 \text{ C}^{-1}$. High-performance multi-color (red–orange, dark green, blue, and purple blue) characteristics of the Mo-doped V_2O_5 thin films were simultaneously obtained. All these results indicate that proper annealing treatment of Mo-doped V_2O_5 thin films is necessary to boost the electrochromic performance.

Acknowledgments This project is supported by the Applied Research Funds for Public Welfare Project of Zhejiang Province (2015C31114), the National Natural Science Foundation of China (51301043, 51302276, and 11474294), and the Natural Science Foundation of Zhejiang Province (LY14E020010).

Open Access This article is distributed under the terms of the Creative Commons Attribution 4.0 International License (<http://creativecommons.org/licenses/by/4.0/>), which permits unrestricted use, distribution, and reproduction in any medium, provided you give appropriate credit to the original author(s) and the source, provide a link to the Creative Commons license, and indicate if changes were made.

References

- Lior N (2013) Mirrors in the sky: status, sustainability, and some supporting materials experiments. *Renew Sustain Energy Rev* 18:401–415
- Jang W-L, Lu Y-M, Chen C-L, Lu Y-R, Dong C-L, Hsieh P-H et al (2014) Local geometric and electronic structures of gasochromic VO_x films. *Phys Chem Chem Phys* 16:4699–4708
- Gillaspie D, Norman A, Tracy CE, Pitts JR, Lee S-H, Dillon A (2010) Nanocomposite counter electrode materials for electrochromic windows. *J Electrochem Soc* 157:H328–H331
- Lee ES, DiBartolomeo D (2002) Application issues for large-area electrochromic windows in commercial buildings. *Sol Energy Mater Sol Cells* 71:465–491
- Vasilyeva SV, Beaujuge PM, Wang S, Babiarz JE, Ballarotto VW, Reynolds JR (2011) Material strategies for black-to-transmissive window-type polymer electrochromic devices. *ACS Appl Mater Interfaces* 3:1022–1032
- Shaplov AS, Ponkratov DO, Aubert P-H, Lozinskaya EI, Plesse C, Maziz A et al (2014) Truly solid state electrochromic devices constructed from polymeric ionic liquids as solid electrolytes and electrodes formulated by vapor phase polymerization of 3,4-ethylenedioxythiophene. *Polymer* 55:3385–3396
- Xu C, Zhao J, Yu J, Cui C (2013) Ethylenedioxythiophene derivatized polynaphthalenes as active materials for electrochromic devices. *Electrochim Acta* 96:82–89
- Somani PR, Radhakrishnan S (2003) Electrochromic materials and devices: present and future. *Mater Chem Phys* 77:117–133
- Yoo SJ, Lim JW, Sung Y-E (2006) Improved electrochromic devices with an inorganic solid electrolyte protective layer. *Sol Energy Mater Sol Cells* 90:477–484
- Wang Z, Chen J, Hu X (2000) Electrochromic properties of aqueous sol–gel derived vanadium oxide films with different thickness. *Thin Solid Films* 375:238–241
- Karuppasamy A (2013) Electrochromism in surface modified crystalline WO₃ thin films grown by reactive DC magnetron sputtering. *Appl Surf Sci* 282:77–83
- Beke S, Giorgio S, Kőrösi L, Nanai L, Marine W (2008) Structural and optical properties of pulsed laser deposited V₂O₅ thin films. *Thin Solid Films* 516:4659–4664
- Wang W, Pang Y, Hodgson SN (2009) XRD studies of thermally stable mesoporous tungsten oxide synthesised by a templated sol-gel process from tungstic acid precursor. *Microporous Mesoporous Mater* 121:121–128
- Minch R, Moonosawmy KR, Solterbeck C-H, Es-Souni M (2014) The influence of processing conditions on the morphology and thermochemical properties of vanadium oxide films. *Thin Solid Films* 556:277–284
- Raj DV, Ponpandian N, Mangalaraj D, Viswanathan C (2013) Effect of annealing and electrochemical properties of sol–gel dip coated nanocrystalline V₂O₅ thin films. *Mater Sci Semicond Process* 16:256–262
- Najdoski M, Koleva V, Samet A (2014) Effect of deposition conditions on the electrochromic properties of nanostructured thin films of ammonium intercalated vanadium pentoxide xerogel. *J Phys Chem C* 118:9636–9646
- Jin A, Chen W, Zhu Q, Yang Y, Volkov V, Zakharova G (2009) Structural and electrochromic properties of molybdenum doped vanadium pentoxide thin films by sol–gel and hydrothermal synthesis. *Thin Solid Films* 517:2023–2028
- Yue Q, Jiang H, Hu Y, Jia G, Li C (2014) Mesoporous single-crystalline V₂O₅ nanorods assembled into hollow microspheres as cathode materials for high-rate and long-life lithium-ion batteries. *Chem Commun* 50:13362–13365
- Yu D, Chen C, Xie S, Liu Y, Park K, Zhou X et al (2011) Mesoporous vanadium pentoxide nanofibers with significantly enhanced Li-ion storage properties by electrospinning. *Energy Environ Sci* 4:858–861
- Zhang X, Sun H, Li Z, Xu J, Jiang S, Zhu Q et al (2013) Synthesis and electrochromic characterization of vanadium pentoxide/graphene nanocomposite films. *J Electrochem Soc* 160:H587–H590
- Su D, Wang G (2013) Single-crystalline bilayered V₂O₅ nanobelts for high-capacity sodium-ion batteries. *ACS Nano* 7:11218–11226
- Wang Y, Li M, Zhao L (2007) The effects of vacuum annealing on the structure of VO₂ thin films. *Surf Coat Technol* 201:6772–6776
- Tepavcevic S, Xiong H, Stamenkovic VR, Zuo X, Balasubramanian M, Prakapenka VB et al (2012) Nanostructured bilayered vanadium oxide electrodes for rechargeable sodium-ion batteries. *ACS Nano* 6:530–538
- Upadhyay SB, Mishra RK, Sahay PP (2015) Enhanced acetone response in co-precipitated WO₃ nanostructures upon indium doping. *Sens Actuators B Chem* 209:368–376
- Guo Y, Xu H, Zou C, Yang Z, Tong B, Yu J et al (2015) Evolution of structure and electrical properties with annealing time in solution-based VO₂ thin films. *J Alloy Compd* 622:913–917
- González-Rivera Y, Cervantes-Juárez E, Aquino-Meneses L, Lozada-Morales R, Jiménez-Sandoval S, Rubio-Rosas E et al (2014) Photoluminescence in Er-doped V₂O₅ and Er-doped CdV₂O₆. *J Lumin* 155:119–124
- Cremonesi A, Bersani D, Lottici P, Djaoued Y, Brüning R (2006) Synthesis and structural characterization of mesoporous V₂O₅ thin films for electrochromic applications. *Thin Solid Films* 515:1500–1505
- Jin A, Chen W, Zhu Q, Jian Z (2010) Multi-electrochromism behavior and electrochromic mechanism of electrodeposited molybdenum doped vanadium pentoxide films. *Electrochim Acta* 55:6408–6414
- Tong Z, Hao J, Zhang K, Zhao J, Su B-L, Li Y (2014) Improved electrochromic performance and lithium diffusion coefficient in three-dimensionally ordered macroporous V₂O₅ films. *J Mater Chem C* 2:3651–3658
- Jeyalakshmi K, Purushothaman K, Muralidharan G (2013) Thickness dependent supercapacitor behaviour of sol-gel spin coated nanostructured vanadium pentoxide thin films. *Phil Mag* 93:1490–1499
- Lu Y, Liu L, Mandler D, Lee PS (2013) High switching speed and coloration efficiency of titanium-doped vanadium oxide thin film electrochromic devices. *J Mater Chem C* 1:7380–7386